Current Biology 24, 753–759, March 31, 2014 ©2014 Elsevier Ltd All rights reserved http://dx.doi.org/10.1016/j.cub.2014.02.024

Report

Inhibitory GEF Phosphorylation Provides Negative Feedback in the Yeast Polarity Circuit

Chun-Chen Kuo,[1] Natasha S. Savage,[2] Hsin Chen,[1,3] Chi-Fang Wu,[1] Trevin R. Zyla,[1] and Daniel J. Lew[1,*]
[1]Department of Pharmacology and Cancer Biology, Duke University Medical Center, Durham, NC 27710, USA
[2]Institute of Integrative Biology, University of Liverpool, Liverpool L69 7ZB, UK

Summary

Cell polarity is critical for the form and function of many cell types. During polarity establishment, cells define a cortical "front" that behaves differently from the rest of the cortex. The front accumulates high levels of the active form of a polarity-determining Rho-family GTPase (Cdc42, Rac, or Rop) that then orients cytoskeletal elements through various effectors to generate the polarized morphology appropriate to the particular cell type [1, 2]. GTPase accumulation is thought to involve positive feedback, such that active GTPase promotes further delivery and/or activation of more GTPase in its vicinity [3]. Recent studies suggest that once a front forms, the concentration of polarity factors at the front can increase and decrease periodically, first clustering the factors at the cortex and then dispersing them back to the cytoplasm [4–7]. Such oscillatory behavior implies the presence of negative feedback in the polarity circuit [8], but the mechanism of negative feedback was not known. Here we show that, in the budding yeast *Saccharomyces cerevisiae*, the catalytic activity of the Cdc42-directed GEF is inhibited by Cdc42-stimulated effector kinases, thus providing negative feedback. We further show that replacing the GEF with a phosphosite mutant GEF abolishes oscillations and leads to the accumulation of excess GTP-Cdc42 and other polarity factors at the front. These findings reveal a mechanism for negative feedback and suggest that the function of negative feedback via GEF inhibition is to buffer the level of Cdc42 at the polarity site.

Results and Discussion

Cdc24 Phosphorylation Reduces GEF Activity In Vitro

Guanosine triphosphate (GTP)-Cdc42 is known to activate p21-activated kinases (PAKs) that then phosphorylate the Cdc42-directed guanine nucleotide exchange factor (GEF) Cdc24 [9, 10]. To assess the effect of phosphorylation on Cdc24 GEF activity, we isolated hemagglutinin (HA) epitope-tagged Cdc24 from yeast cells that overexpressed the protein, and then we measured its ability to stimulate guanosine diphosphate (GDP)/GTP exchange on recombinant Cdc42 (Figure 1A). HA-Cdc24 displayed robust GEF activity that was abolished by mutations in the catalytic domain, indicating that the activity was intrinsic to Cdc24 and not due to a coprecipitating factor (Figure 1B). As judged by gel mobility, a majority of the HA-Cdc24 was not phosphorylated. To generate a preparation of highly phosphorylated Cdc24, we coexpressed the activated Cdc42 mutant $Cdc42^{Q61L}$ and a Bem1-Cla4 fusion protein [11] to promote Cla4 (PAK)-mediated hyperphosphorylation of HA-Cdc24 (Figure 1C). Phosphorylated Cdc24 was less active than unphosphorylated Cdc24 (Figure 1D). This was due to phosphorylation, because treatment with λ phosphatase caused an increase in GEF activity (Figure 1E). We conclude that Cdc24 phosphorylation reduces GEF activity.

GEF activity was reduced ~2-fold for phosphorylated versus unphosphorylated Cdc24 preparations (Figures 1D and 1E). However, the phosphorylated preparation exhibited a heterogeneous mixture of phosphorylation states (Figures 1D and 1E, insets), due to partial dephosphorylation during immunoprecipitation and washing. Because 40%–50% of the "phosphorylated" protein migrated at a comparable position to unphosphorylated Cdc24, it may be that all remaining activity stems from that less phosphorylated subset and that the highly phosphorylated Cdc24 is completely inactive.

Assay for Cdc24 Activity In Vivo

To assess Cdc24 activity in vivo, we followed a strategy based on the expectation that if Cdc24 were targeted uniformly to the plasma membrane (rather than just to the polarity site), then it would generate GTP-Cdc42 all over the membrane (Figure 2A). In turn, that should dominantly interfere with polarization mediated by the endogenous Cdc24, blocking proliferation [12]. The level of expression needed to block polarization would depend on the activity of the membrane-targeted Cdc24 (MT-Cdc24), providing a measure for Cdc24 activity in vivo. We used a 28-residue N-terminal peptide from Psr1 [13] to efficiently target Cdc24 to the plasma membrane. Levels of expression were controlled by an estrogen-inducible promoter system (Figure 2A) [14]. High-level expression of MT-Cdc24 induced accumulation of GTP-Cdc42 all over the plasma membrane (Figure 2B) and blocked both polarization (Figure 2B) and proliferation (Figure 2D).

In principle, the effect of MT-Cdc24 could stem from its catalytic activity (promoting uniform cortical GTP-Cdc42 accumulation), or from titrating Cdc24 interactors (e.g., Bem1 [15] and Rsr1-GTP [16]) away from the endogenous Cdc24, or both. We found that a membrane-targeted but catalytically dead Cdc24 (MT-Cdc24-AA) was no longer effective in promoting accumulation of GTP-Cdc42 all over the membrane (Figures 2B and 2C) but was still able to block proliferation at high expression levels, presumably via titration (Figure 2D). Membrane targeting of a Bem1-binding-deficient mutant (MT-Cdc24-KR: D824K, D831R [17]) was also able to block proliferation at high expression levels (Figure 2D). At lower expression levels, only MT-Cdc24 (and not MT-Cdc24-AA or MT-Cdc24-KR) blocked proliferation (Figure 2D). A double mutant lacking both catalytic activity and Bem1-binding ability did not block proliferation (Figure 2D). Thus, the polarity-blocking effect of MT-Cdc24 reflects additive contributions from its catalytic activity and from Bem1 titration.

[3]Present address: Howard Hughes Medical Institute and Department of Microbiology and Immunology, University of California, San Francisco, San Francisco, CA 94143, USA
*Correspondence: daniel.lew@duke.edu

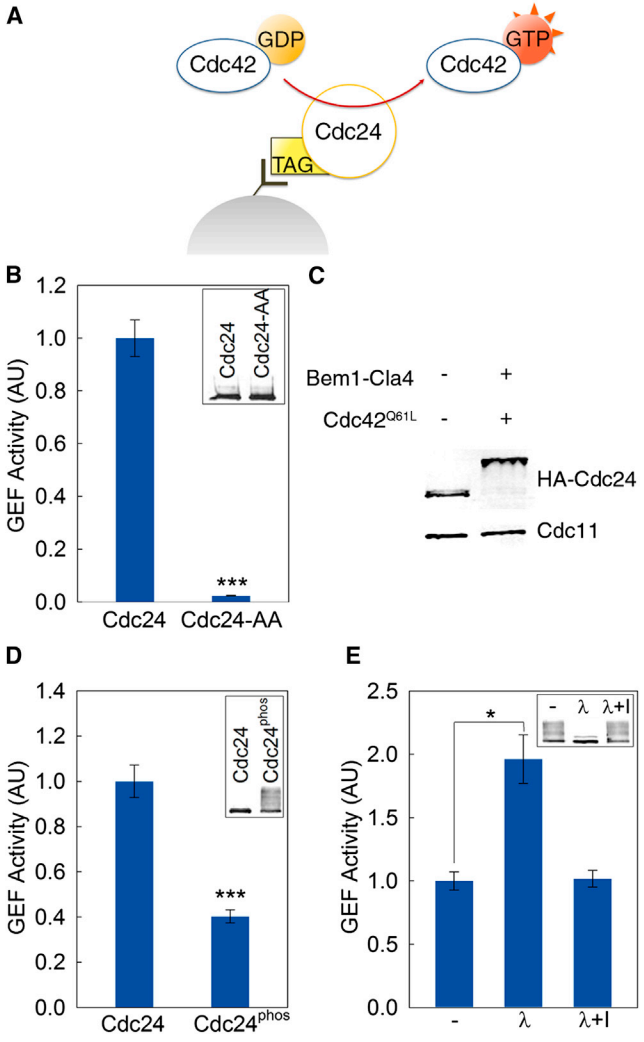

Figure 1. GEF Phosphorylation Inhibits Activity

(A) Measurement of Cdc24 GEF activity in vitro. Immunoprecipitated HA-Cdc24 isolated from yeast is incubated with recombinant GDP-Cdc42 and γ-^{35}S-GTP. GTP loading is assessed by a filtration assay.

(B) Cdc42 GTP loading by wild-type Cdc24 or a catalytic domain mutant N452A/E453A (designated Cdc24-AA). Arbitrary units (AU) represent the amount of radioactive GTP loaded divided by the amount of HA-Cdc24 in the immunoprecipitate (inset). Activity is normalized to the wild-type Cdc24 sample. Mean ± SEM is shown (n = 3).

(C) Western blot of Cdc24 isolated from wild-type cells (DLY15284) or cells overexpressing Cdc42^{Q61L} and Bem1-Cla4 (DLY15332). The latter (designated Cdc24^{Phos}) shows a mobility shift, indicating hyperphosphorylation. Cdc11 is the loading control.

(D) Cdc24^{Phos} has reduced GEF activity. Assay was as in (B). Mean ± SEM is shown (n = 4).

(E) Phosphatase treatment of Cdc24^{Phos} increases GEF activity. Cdc24^{Phos} was treated with buffer, λ phosphatase, or λ phosphatase plus phosphatase inhibitors, as indicated. Assay was as in (B). Mean ± SEM is shown (n = 3). ***p < 0.001, *p < 0.02 (two-tailed t test).

Nonphosphorylatable Cdc24 Is Hyperactive In Vivo

MT-Cdc24 exhibited a gel mobility shift compared with wild-type Cdc24, and phosphatase treatment reversed the shift (Figure 2E), suggesting that MT-Cdc24 is highly phosphorylated. A previous study mapped 35 phosphorylation sites on Cdc24 using mass spectrometry and generated a "nonphosphorylatable" Cdc24^{38A} mutant that lacked those sites and an additional three putative sites (although this mutant was still phosphorylated at a few additional sites, as judged by gel mobility) [18]. We generated a version of MT-Cdc24 containing 33 of those 38 phosphorylation-site mutations (the most N-terminal four mutations and most C-terminal mutation were omitted by the cloning strategy). We also generated variants harboring only seven mutations (at designated "PAK consensus sites" [18]) or only four mutations (at designated "CDK consensus sites" [18]). Compared with MT-Cdc24, MT-Cdc24^{33A} exhibited a much smaller mobility shift, whereas MT-Cdc24^{7A} and MT-Cdc24^{4A} were still highly phosphorylated (Figure 2F). MT-Cdc24^{33A} (but not MT-Cdc24^{7A} or MT-Cdc24^{4A}) was more effective at blocking proliferation than MT-Cdc24 (Figure 2F). MT-Cdc24^{33A} was also more effective at promoting uniform GTP-Cdc42 accumulation (Figures 2B and 2C), suggesting that it had greater catalytic activity. To assess whether the enhanced potency of MT-Cdc24^{33A} in blocking proliferation was due solely to enhanced catalytic activity, we generated a nonphosphorylatable but catalytically dead MT-Cdc24^{33A}-AA mutant. This construct was no more effective than MT-Cdc24-AA at inducing cortical GTP-Cdc42 accumulation (Figures 2B and 2C) or blocking proliferation (Figure 2G). Thus, mutation of most of the mapped Cdc24 phosphorylation sites increased the catalytic activity of MT-Cdc24 in vivo, leading to a more potent block in proliferation.

MT-Cdc24^{33A} also had more GEF activity than the highly phosphorylated MT-Cdc24 in vitro (Figure 2H). In principle, the increased activity could be due either to the lack of phosphorylation or to some conformational effect of the mutations themselves. To distinguish between these possibilities, we generated a comparable GFP-Cdc24^{33A} that lacked the membrane-targeting Psr1 domain. In the absence of membrane targeting, overexpressed GFP-Cdc24 is almost all cytoplasmic (Figure 2B) and unphosphorylated (Figure 1B). In that context, Cdc24^{33A} had no more GEF activity than unphosphorylated Cdc24 (Figure 2I). Thus, the increased activity of MT-Cdc24^{33A} is due to the absence of phosphorylation. We conclude that Cdc24 phosphorylation reduces GEF activity in vivo and in vitro.

Cdc24 phosphorylation was reported to abolish Cdc24-Bem1 interaction [9]. However, we found that immunoprecipitated Bem1-myc associated with both phosphorylated MT-Cdc24 and unphosphorylated Cdc24 (Figure 3A). Similarly, phosphorylated MT-Cdc24 and unphosphorylated Cdc24 both associated with comparable amounts of Bem1-myc (Figure 3B). Thus, we see no strong effect of Cdc24 phosphorylation on Bem1 binding.

Because the activity of isolated Cdc24 was increased by phosphatase treatment in vitro (under conditions where that could not be due to an increase in Bem1 binding; Figure 1E), we conclude that Cdc24 phosphorylation directly affects catalytic activity, independently of Bem1 binding. Combined with previous studies [9, 10], our finding that phosphorylation of Cdc24 inhibits its catalytic activity reveals a negative feedback pathway acting in the yeast polarity circuit. The pathway involves the following steps: (1) GTP-Cdc42 activates PAKs, (2) PAKs phosphorylate Cdc24, (3) phosphorylation inhibits Cdc24 GEF activity, and (4) reduced GEF activity leads to lower levels of GTP-Cdc42.

Computational Modeling of Negative Feedback through Cdc24 Phosphorylation

Because polarization can be initiated by stochastic fluctuations, which can occur at multiple locations, cells often begin

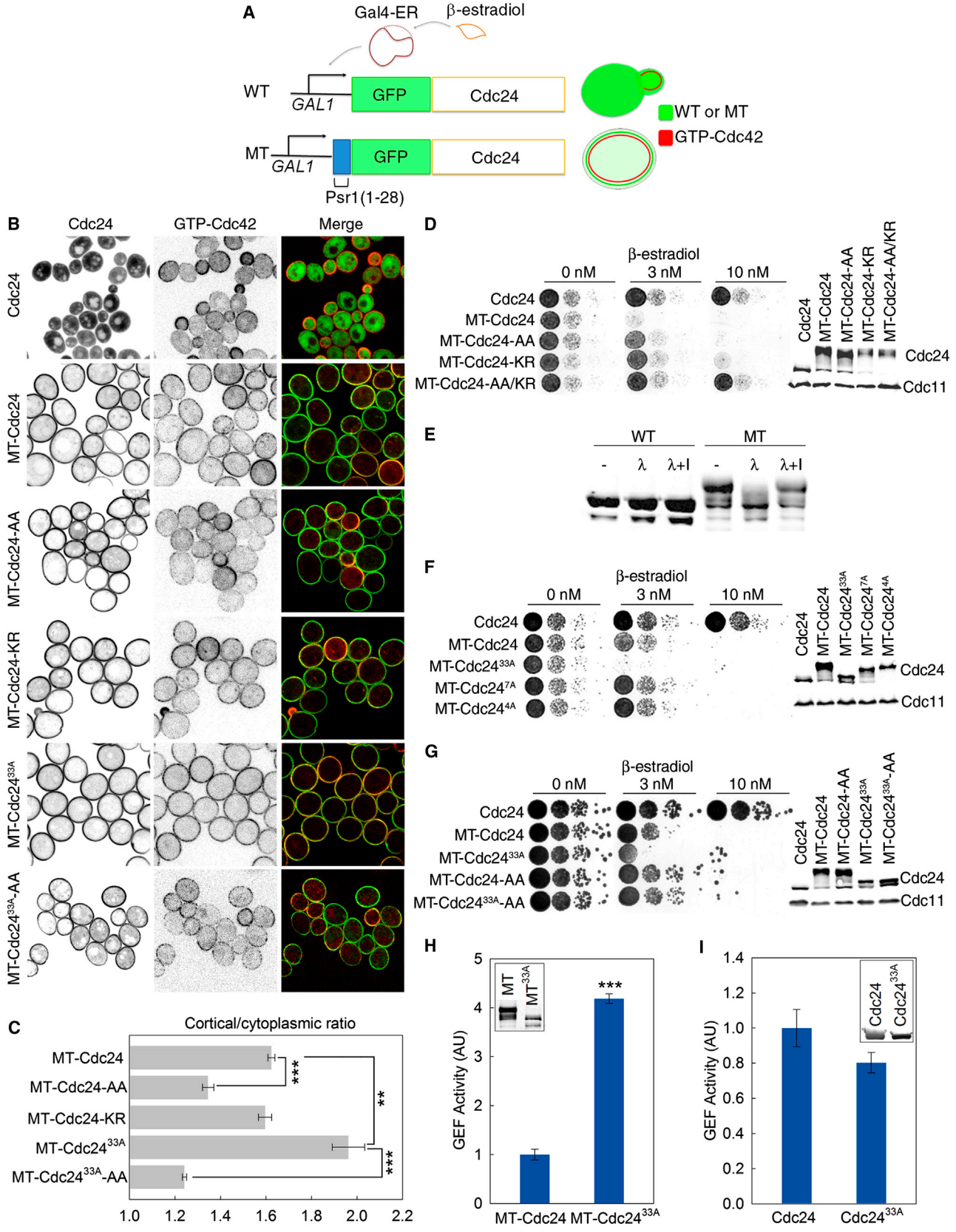

Figure 2. Phosphosite Mutant GEF Is More Active In Vivo

(A) Assay for Cdc24 activity in vivo. An estradiol-regulated derivative of Gal4 (Gal4-ER) allows graded induction of the *GAL1* promoter, driving overexpression of wild-type (WT) or MT GFP-Cdc24. WT Cdc24 is mostly cytoplasmic, and overexpression is well tolerated: cells polarize GTP-Cdc42 and

(legend continued on next page)

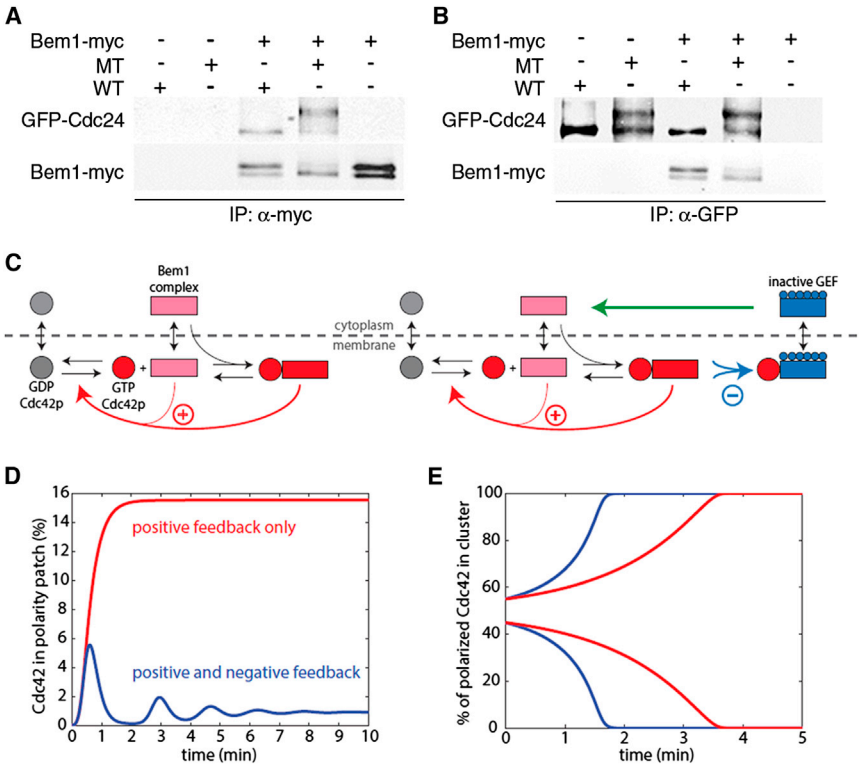

Figure 3. GEF Phosphorylation Does Not Affect Bem1 Binding; Modeling Negative Feedback

(A) Immunoprecipitated Bem1-myc associates with both phosphorylated MT-Cdc24 and unphosphorylated Cdc24. IP, immunoprecipitate.

(B) Immunoprecipitated MT-Cdc24 and WT Cdc24 associate with comparable amounts of Bem1-myc.

(C) Schematic of models with and without negative feedback. In both models, the Bem1 complex can associate with GTP-Cdc42, and load GTP on neighboring GDP-Cdc42, providing positive feedback. Negative feedback is modeled as a transition of the Cdc42-bound Bem1 complex to an inactive, phosphorylated form (blue) that can dissociate from Cdc42 and be dephosphorylated in the cytoplasm.

(D) Simulations of polarity establishment using the two models. The amount of Cdc42 (percent of total) at the polarity site increases to a high plateau in the model with only positive feedback (red). Addition of negative feedback reduces Cdc42 accumulation and yields damped oscillations before reaching a low steady state (compared to the peak).

(E) Simulations of competition between two polarity clusters at opposite ends of the cell. Simulations were initiated with clusters containing Cdc42 at a 45:55 ratio, and the upper lines show growth of the winning clusters, whereas the lower lines show disappearance of the losing clusters. Competition is resolved more rapidly with (blue) than without (red) negative feedback.

to concentrate Cdc42 at more than one site [6, 19]. However, Cdc42 clusters then appear to compete with each other, so that one cluster grows to become the front while all of the other clusters disappear [6, 20]. Theoretical studies have shown that the known biochemical interactions and activities of Cdc42, the PAK-Bem1-Cdc24 complex, and a guanine nucleotide dissociation inhibitor are sufficient in principle to explain both clustering of polarity factors and competition between clusters [20, 21]. To explain oscillatory clustering, an additional negative feedback loop was posited [6], although the mechanism of negative feedback was unknown.

Given our findings, we asked whether adding inhibitory multisite phosphorylation of Cdc24 to the previous positive-feedback-only model (Figure 3C) could produce oscillatory clustering. Because multisite phosphorylation can yield ultrasensitive behavior [22–24], we modeled phosphorylation as a Hill function of the concentration of Cdc42-bound Bem1 complexes (see "Computational Modeling" in the Supplemental Experimental Procedures). However, ultrasensitivity was not essential to produce the predictions discussed below.

Simulations incorporating negative feedback displayed dampened oscillations, as well as reduced Cdc42 accumulation at the polarity site (Figure 3D). We also simulated cells in which two slightly unequal polarity clusters were formed at opposite ends of the cell and followed the relative amount of Cdc42 in each cluster. Competition was resolved more rapidly in simulations containing negative feedback (Figure 3E). Thus, if the model approximates the true situation in cells, then short-circuiting the negative feedback loop by rendering Cdc24 nonphosphorylatable should abolish oscillations, increase Cdc42 levels at the front, and slow down competition between clusters.

form buds (top). A lipid-modified Psr1 peptide (blue) targets MT-Cdc24 uniformly around the plasma membrane, leading to uniform GTP-Cdc42 accumulation, loss of polarity, and failure to proliferate (bottom).

(B) Localization of the GTP-Cdc42 probe Gic2$^{1–208}$-tdTomato in cells overexpressing WT or MT GFP-Cdc24 derivatives. Cells overexpressing the indicated versions of Cdc24 were treated with 50 nM β-estradiol for 3–4 hr, and single confocal planes were imaged (GFP, left; RFP, middle; merge, right). All MT versions blocked polarization at this high level of expression, leading to accumulation of large unbudded cells.

(C) Quantification of the cortical-to-cytoplasmic fluorescence ratio for the GTP-Cdc42 probe in cells expressing MT-Cdc24 derivatives. Mean ± SEM is shown (n = 5 fields of cells with ~40 cells/field). ***p < 0.001, **p < 0.01 (two-tailed t test). Cortical Cdc42 was reduced by catalytic mutations but increased by phosphosite mutations.

(D) MT-Cdc24 overexpression blocks proliferation by a combination of catalytic activity and Bem1 titration. Left: cells were spotted (10-fold serial dilutions) onto plates containing the indicated concentrations of β-estradiol to induce expression of Cdc24 or MT-Cdc24 derivatives and then incubated for 2 days at 24°C. MT-Cdc24-AA can titrate Bem1 but lacks catalytic activity, whereas MT-Cdc24-KR has catalytic activity but cannot titrate Bem1: both block proliferation, but less effectively than MT-Cdc24. Right: blot shows levels of induction (MT-Cdc24 has slower mobility due to phosphorylation). Cdc11 is the loading control.

(E) MT-Cdc24 is highly phosphorylated. Mobility shift is reduced upon treatment with λ phosphatase, but not λ phosphatase plus phosphatase inhibitors.

(F) MT-Cdc24^{33A} is more potent at blocking proliferation than MT-Cdc24. Assay and blots were as in (D).

(G) Catalytically dead MT-Cdc24^{33A} is comparable at blocking proliferation to catalytically dead MT-Cdc24. Assay and blots were as in (D).

(H) MT-Cdc24^{33A} displays higher GEF activity than MT-Cdc24. Assays were as in Figure 1B, except that the GEF was immunoprecipitated using anti-GFP. Mean ± SEM is shown (n = 3). ***p < 0.001 (two-tailed t test).

(I) Cdc24, which is largely unphosphorylated when overexpressed, has comparable GEF activity to Cdc24^{33A}. Mean ± SEM is shown (n = 3).

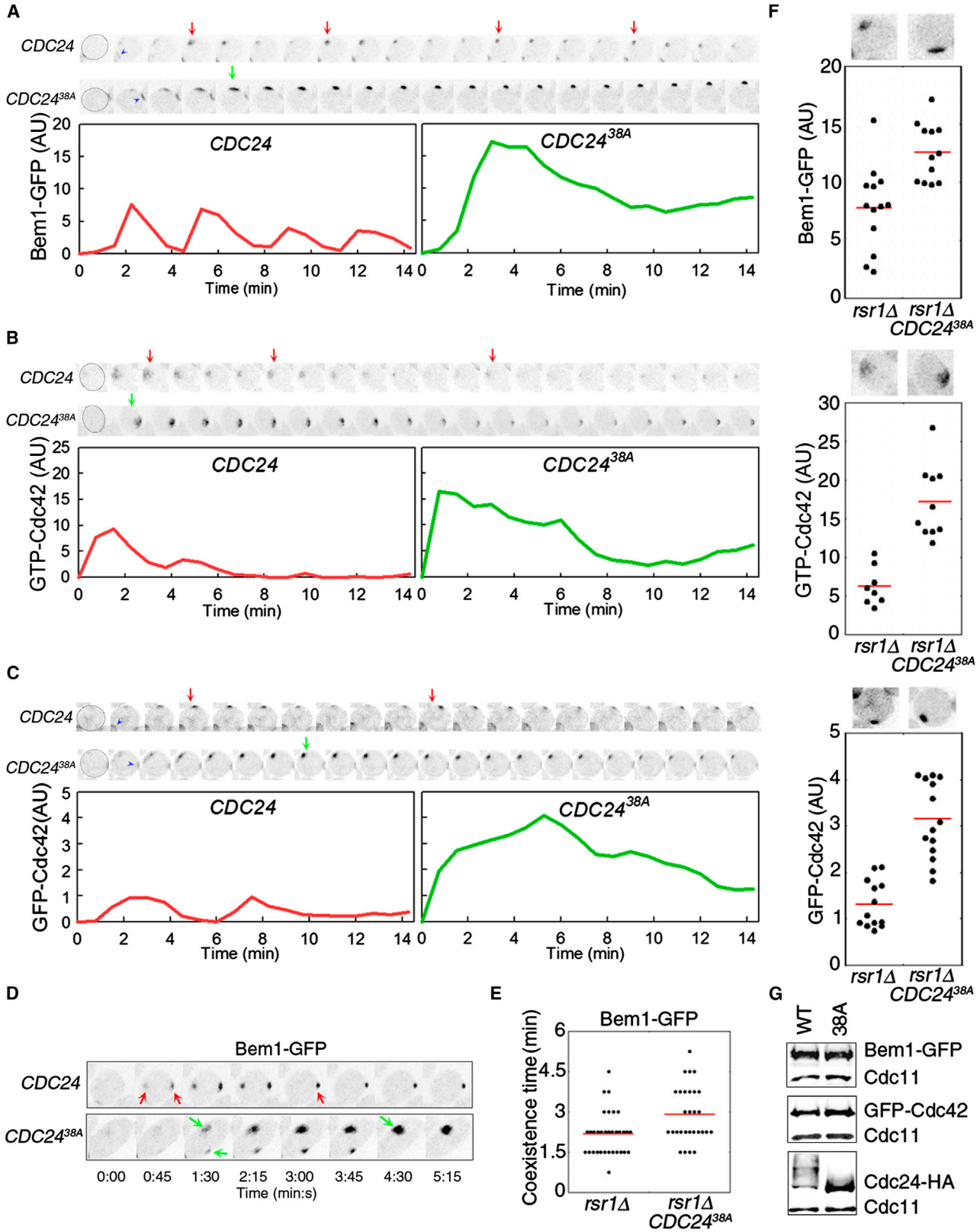

Figure 4. Negative Feedback via GEF Phosphorylation Promotes Oscillatory Clustering and Lowers GTP-Cdc42 Levels at the Polarity Site

(A) Dynamics of Bem1-GFP clustering in *CDC24* and *CDC24*^{38A} cells. Cells were imaged side by side to allow direct comparison of Bem1-GFP intensities. Maximum projections of confocal stacks are shown, and intensity of the probe in the cluster is quantitated. Blue arrowhead, signal from old neck or neighboring cell (not polarity site). Arrows show clustering peak(s): red, *CDC24* cells (control); green, *CDC24*^{38A} cells.

(B) Dynamics of GTP-Cdc42 clustering visualized with Gic2$^{1–208}$-tdTomato, as in (A).

(legend continued on next page)

Cdc24 Phosphorylation Is Required for Oscillatory Polarization but Does Not Affect Competition between Polarity Clusters

Previous work showed that nonphosphorylatable Cdc24^{38A} was functional, but the dynamics of polarization was not examined [18]. We generated yeast strains in which endogenous *CDC24* was precisely replaced by *CDC24*^{38A} at its endogenous locus and monitored polarization using Bem1-GFP [11], GFP-Cdc42, or the GTP-Cdc42 reporter Gic2$^{1–208}$-tdTomato [25] as probes. We focused on diploid cells lacking the bud-site-selection protein Rsr1, where we had observed oscillatory cycles of clustering and dispersal of polarity factors [6]. Control experiments with HA-tagged constructs showed that Cdc24^{38A} was expressed at similar levels to Cdc24 (Figure 4G), as reported previously [18].

During initial polarity establishment, *CDC24* cells displayed oscillations in the concentration of polarity factors at the front (Figures 4A–4C; Figure S1 available online; Movie S1), as reported previously [6]. In contrast, *CDC24*^{38A} cells kept polarity protein levels high at the front, without discernible oscillations (Figures 4A–4C; Figure S1; Movie S2). Unlike in the model with no negative feedback (Figure 3D), however, levels of polarity factors did gradually decline from the peak in mutant cells (Figures 4A–4C; Figure S1), perhaps reflecting additional sources of negative feedback. Two other negative feedback loops were recently proposed to act through the cytoskeletal targets of Cdc42: actin [26, 27] and septins [28]. These slower feedback loops cannot account for the rapid oscillations [6], but they may contribute to the slower decline in polarity protein levels at the front observed in the *CDC24*^{38A} mutants.

As with *CDC24* cells, several of the *CDC24*^{38A} cells we imaged initially developed more than one polarity cluster (Figure 4D; Movie S2). To assess whether competition between clusters was altered in the mutant cells, we measured the coexistence time (the interval for which two or more clusters were present) for this subset of cells. Quantification indicated that competition timing was generally similar in *CDC24* versus *CDC24*^{38A} cells (Figure 4E). Thus, Cdc24 phosphorylation does not seem to be required to enforce rapid competition.

Cdc24 Phosphorylation Lowers Polarity Factor Concentrations at the Front

To compare the relative intensity of polarized signals, *CDC24* and *CDC24*^{38A} cells were imaged side by side on the same slide (Movie S3). Peak levels of Bem1, Cdc42, and GTP-Cdc42 were all higher in *CDC24*^{38A} cells than in *CDC24* cells (Figure 4F). This was not due to an increase in total cellular levels of Bem1 or Cdc42 (Figure 4G). The effect of *CDC24*^{38A} was dominant to wild-type, as expected for a hyperactive protein (Figure S1D). Thus, negative feedback through Cdc24 phosphorylation acts to reduce polarity factor accumulation at the cortex.

CDC24^{38A} cells did not display any major changes in polarization efficiency, proliferation rate, or cell morphology. Thus, it appears that cells can tolerate increased levels of polarized GTP-Cdc42 without severe ill effects, at least under lab growth conditions. Negative feedback may become more important when polarity-affecting stresses occur in more physiological environments. Alternatively, like cell-cycle checkpoints and DNA repair pathways, negative feedback may only be critical for a minority of cells that experience polarity problems (e.g., because they contain potentially dangerous levels of polarity factors). Consistent with that hypothesis, preliminary observations suggest that negative feedback becomes important for proliferation when Cdc42 is overexpressed. It will be of great interest to determine whether polarity establishment in other systems also employs inhibitory GEF phosphorylation to regulate polarization.

Supplemental Information

Supplemental Information includes Supplemental Experimental Procedures, one figure, and three movies and can be found with this article online at http://dx.doi.org/10.1016/j.cub.2014.02.024.

Acknowledgments

We thank Denis Tsyganov for providing the image analysis tool to quantify the cortical-to-cytoplasmic fluorescence ratio. We thank Nick Buchler, Steve Haase, Tim Elston, and members of the Lew lab for stimulating discussions and feedback on the manuscript. We thank M. Peter (ETH, Zurich, Switzerland) for the gift of the HA-Cdc24 plasmid, and S. Smith and R. Li (Stowers Institute, Kansas City, MO) for the gift of phospho-site mutant Cdc24. Funding was provided by a fellowship from the National Science Council of Taiwan to C.-C.K., a Wellcome Trust ISSF fellowship to N.S.S., and NIH/NIGMS grant GM62300 to D.J.L.

Received: October 7, 2013
Revised: January 21, 2014
Accepted: February 11, 2014
Published: March 13, 2014

References

1. Etienne-Manneville, S. (2004). Cdc42—the centre of polarity. J. Cell Sci. *117*, 1291–1300.
2. Yang, Z., and Lavagi, I. (2012). Spatial control of plasma membrane domains: ROP GTPase-based symmetry breaking. Curr. Opin. Plant Biol. *15*, 601–607.
3. Johnson, J.M., Jin, M., and Lew, D.J. (2011). Symmetry breaking and the establishment of cell polarity in budding yeast. Curr. Opin. Genet. Dev. *21*, 740–746.
4. Hwang, J.U., Gu, Y., Lee, Y.J., and Yang, Z. (2005). Oscillatory ROP GTPase activation leads the oscillatory polarized growth of pollen tubes. Mol. Biol. Cell *16*, 5385–5399.
5. Carlin, L.M., Evans, R., Milewicz, H., Fernandes, L., Matthews, D.R., Perani, M., Levitt, J., Keppler, M.D., Monypenny, J., Coolen, T., et al. (2011). A targeted siRNA screen identifies regulators of Cdc42 activity at the natural killer cell immunological synapse. Sci. Signal. *4*, ra81.
6. Howell, A.S., Jin, M., Wu, C.F., Zyla, T.R., Elston, T.C., and Lew, D.J. (2012). Negative feedback enhances robustness in the yeast polarity establishment circuit. Cell *149*, 322–333.
7. Das, M., Drake, T., Wiley, D.J., Buchwald, P., Vavylonis, D., and Verde, F. (2012). Oscillatory dynamics of Cdc42 GTPase in the control of polarized growth. Science *337*, 239–243.

(C) Dynamics of GFP-Cdc42 clustering, as in (A).
(D) Rapid competition in *CDC24* and *CDC24*^{38A} cells that initially form more than one cluster.
(E) Quantification of the time taken to resolve multicluster intermediates in *CDC24* and *CDC24*^{38A} cells.
(F) Quantification of peak Bem1-GFP, Gic2$^{1–208}$-tdTomato, and GFP-Cdc42 intensities in *CDC24* and *CDC24*^{38A} cells. In each case, mutant cells showed a statistically significant ($p < 0.001$) increase in peak levels.
For (E) and (F), each dot is one cell taken from movies as in (A)–(D); the line indicates average.
(G) Levels of HA-Cdc24 and HA-Cdc24^{38A} are comparable, as are total Bem1-GFP and GFP-Cdc42 probes in *CDC24* and *CDC24*^{38A} cells. Cdc11 is the loading control.
See also Figure S1 for more examples from (A)–(C) and Movies S1, S2, and S3.

8. Wu, C.F., and Lew, D.J. (2013). Beyond symmetry-breaking: competition and negative feedback in GTPase regulation. Trends Cell Biol. *23*, 476–483.
9. Gulli, M.P., Jaquenoud, M., Shimada, Y., Niederhäuser, G., Wiget, P., and Peter, M. (2000). Phosphorylation of the Cdc42 exchange factor Cdc24 by the PAK-like kinase Cla4 may regulate polarized growth in yeast. Mol. Cell *6*, 1155–1167.
10. Bose, I., Irazoqui, J.E., Moskow, J.J., Bardes, E.S., Zyla, T.R., and Lew, D.J. (2001). Assembly of scaffold-mediated complexes containing Cdc42p, the exchange factor Cdc24p, and the effector Cla4p required for cell cycle-regulated phosphorylation of Cdc24p. J. Biol. Chem. *276*, 7176–7186.
11. Kozubowski, L., Saito, K., Johnson, J.M., Howell, A.S., Zyla, T.R., and Lew, D.J. (2008). Symmetry-breaking polarization driven by a Cdc42p GEF-PAK complex. Curr. Biol. *18*, 1719–1726.
12. Shimada, Y., Wiget, P., Gulli, M.P., Bi, E., and Peter, M. (2004). The nucleotide exchange factor Cdc24p may be regulated by autoinhibition. EMBO J. *23*, 1051–1062.
13. Siniossoglou, S., Hurt, E.C., and Pelham, H.R. (2000). Psr1p/Psr2p, two plasma membrane phosphatases with an essential DXDX(T/V) motif required for sodium stress response in yeast. J. Biol. Chem. *275*, 19352–19360.
14. Takahashi, S., and Pryciak, P.M. (2008). Membrane localization of scaffold proteins promotes graded signaling in the yeast MAP kinase cascade. Curr. Biol. *18*, 1184–1191.
15. Peterson, J., Zheng, Y., Bender, L., Myers, A., Cerione, R., and Bender, A. (1994). Interactions between the bud emergence proteins Bem1p and Bem2p and Rho-type GTPases in yeast. J. Cell Biol. *127*, 1395–1406.
16. Zheng, Y., Bender, A., and Cerione, R.A. (1995). Interactions among proteins involved in bud-site selection and bud-site assembly in Saccharomyces cerevisiae. J. Biol. Chem. *270*, 626–630.
17. Ito, T., Matsui, Y., Ago, T., Ota, K., and Sumimoto, H. (2001). Novel modular domain PB1 recognizes PC motif to mediate functional protein-protein interactions. EMBO J. *20*, 3938–3946.
18. Wai, S.C., Gerber, S.A., and Li, R. (2009). Multisite phosphorylation of the guanine nucleotide exchange factor Cdc24 during yeast cell polarization. PLoS ONE *4*, e6563.
19. Wu, C.F., Savage, N.S., and Lew, D.J. (2013). Interaction between bud-site selection and polarity-establishment machineries in budding yeast. Philos. Trans. R. Soc. Lond. B Biol. Sci. *368*, 20130006.
20. Howell, A.S., Savage, N.S., Johnson, S.A., Bose, I., Wagner, A.W., Zyla, T.R., Nijhout, H.F., Reed, M.C., Goryachev, A.B., and Lew, D.J. (2009). Singularity in polarization: rewiring yeast cells to make two buds. Cell *139*, 731–743.
21. Goryachev, A.B., and Pokhilko, A.V. (2008). Dynamics of Cdc42 network embodies a Turing-type mechanism of yeast cell polarity. FEBS Lett. *582*, 1437–1443.
22. Nash, P., Tang, X., Orlicky, S., Chen, Q., Gertler, F.B., Mendenhall, M.D., Sicheri, F., Pawson, T., and Tyers, M. (2001). Multisite phosphorylation of a CDK inhibitor sets a threshold for the onset of DNA replication. Nature *414*, 514–521.
23. Strickfaden, S.C., Winters, M.J., Ben-Ari, G., Lamson, R.E., Tyers, M., and Pryciak, P.M. (2007). A mechanism for cell-cycle regulation of MAP kinase signaling in a yeast differentiation pathway. Cell *128*, 519–531.
24. Trunnell, N.B., Poon, A.C., Kim, S.Y., and Ferrell, J.E., Jr. (2011). Ultrasensitivity in the regulation of Cdc25C by Cdk1. Mol. Cell *41*, 263–274.
25. Tong, Z., Gao, X.D., Howell, A.S., Bose, I., Lew, D.J., and Bi, E. (2007). Adjacent positioning of cellular structures enabled by a Cdc42 GTPase-activating protein-mediated zone of inhibition. J. Cell Biol. *179*, 1375–1384.
26. Savage, N.S., Layton, A.T., and Lew, D.J. (2012). Mechanistic mathematical model of polarity in yeast. Mol. Biol. Cell *23*, 1998–2013.
27. Ozbudak, E.M., Becskei, A., and van Oudenaarden, A. (2005). A system of counteracting feedback loops regulates Cdc42p activity during spontaneous cell polarization. Dev. Cell *9*, 565–571.
28. Okada, S., Leda, M., Hanna, J., Savage, N.S., Bi, E., and Goryachev, A.B. (2013). Daughter cell identity emerges from the interplay of Cdc42, septins, and exocytosis. Dev. Cell *26*, 148–161.